Microscopic description of the low-temperature anomalies in silica and lithium silicate via computer simulations

J. Reinisch and A. Heuer

Westfälische Wilhelms-Universität Münster, Institut für Physikalische Chemie

Corrensstr. 30, 48149 Münster, Germany

(Dated: February 6, 2008)

Abstract

Information about the nature of the low-temperature anomalies and in particular the properties of the tunneling systems in silica and lithium silica glasses are revealed via computer simulations. The potential energy landscape of these systems is systematically explored for adjacent pairs of local minima which may act as double-well potentials (DWP) at low temperatures. Three different types of DWP are distinguished, related to perfectly coordinated silica, intrinsic silica defects, and extrinsic defects. Their properties like the spatial extension and the dipole moment are characterized in detail. Furthermore, the absolute number of tunneling systems, i.e. symmetric DWP, is estimated. The results are compared with dielectric echo, specific heat and acoustic experiments on Suprasil I and Suprasil W. A semi-quantitative agreement for all relevant features is obtained.

INTRODUCTION

For more than thirty years it is known that glasses display anomalous behavior for temperatures in the Kelvin regime.[1] For example, the temperature dependence of the specific heat turns out to be linear rather than cubic, as expected from the Debye model. The standard tunneling model (STM) predicts many of these features.[2,3] The key idea is to assume that the system can perform local transitions between adjacent configurations. Because of the low temperatures the crossing of the barriers occurs via tunneling. This feature can be characterized by a double-well potential (DWP) in configuration space, i.e. two adjacent local minima on the potential energy landscape (PEL). In general, the reaction coordinate corresponds to a highly cooperative process in which a group of neighboring atoms is involved. Among all DWP which are present in a given glassy configuration only those DWP with asymmetries less than, let's say, 2 K will contribute to the low-temperature anomalies. In contrast, typical energy scales for, e.g., SiO_2 are of the order of 1eV and thus many orders of magnitude higher. Thus one would expect that only a minor fraction of all DWP are relevant for the low-temperature anomalies. They are denoted two-level systems (TLS).

There is no theory which predicts the properties of TLS from first principles without invoking some model assumptions. There are, however, interesting approaches within different physical frameworks like a mean-field model [4] and random first order transition theory.[5] In the second approach a detailed picture of the PEL in terms of mosaics is derived. In their model the reaction coordinate of TLS involves the dynamics of $O(10^2)$ molecules which only move a small fraction of a nearest-neighbor distance. Finally, in the STM some reasonable assumptions about the properties of the potential parameters of the TLS are made.

Computer simulations are well suited to elucidate the properties of TLS. Two steps are involved. First, one has to generate a typical glassy configuration and, second, to identify nearby adjacent minima on the PEL and characterize the nature of the individual transitions. Qualitatively, one would expect that the active atoms for one transition are localized in some region in the glass. The first simulations used non-systematic search methods.[6,7] In subsequent work Heuer and Silbey have introduced a method how to search TLS in a systematic way.[8] Applying this method to a binary mixture Lennard-Jones (BMLJ) system they were able to predict the real-space realization of the TLS [8], the coupling to strain, [9,10] the prediction of tunneling properties in terms of material constants and, as a consequence,

a universal description of the low-temperature anomalies.[11,12] Important results about the properties of DWP in Lennard-Jones systems can be also found in Refs. [13–15]. For all simulations one has to take into account that the absolute number of TLS is so small that there is no chance to identify a sufficiently large number via simulations. In contrast, the number of DWP is very large. Therefore an important ingredient of these simulations is the formulation of a statistical method how to predict the properties of TLS from those of DWP. Using the significantly improved computer facilities during the last decade, the present authors have recently reanalyzed the BMLJ system .[16,17] In particular, it could be shown that (1) the systematic search algorithm indeed allows one to obtain an estimation of the absolute number of TLS, (2) the properties of the TLS basically do not depend on the energy of the configuration. Thus, the intrinsic computer limitations like the necessity of a very fast cooling procedure to generate the initial configuration or the choice of relatively small systems do not hamper the unbiased determination of TLS properties in the BMLJ system.

A prototype glass-forming system is vitreous silica (SiO_2). Trachenko et al have characterized the TLS of silica in several respects and have shown that the microscopic nature is related to coupled rotations of SiO_4 tetrahedra.[18–21] A similar picture has been suggested from experimental neutron data [22] and from the analysis of localized vibrational modes. [23] The transition events have been also analyzed via the activation-relaxation technique.[24] The present authors have conducted a systematic search for TLS in silica.[25] It has been possible to estimate the experimentally observed number of TLS which has turned out to be a factor of approx. 3 smaller than the experimental TLS density reported for Suprasil W. As argued in Ref.[25] there are two possible reasons for a slight underestimation by computer simulations which are connected with the estimation of the tunneling matrix element. Going beyond the WKB-approximation one might additionally take into account that (i) the saddles are broader (in terms of second derivatives) than the minima (see also Refs.[14,17]) and (ii) there is a Franck-Condon factor, taking into account the relaxation of the phonon modes during the transition within a DWP.[17] Both effects would increase the estimation of the number of TLS and might at least partly account for the remaining difference.

In general, one may distinguish intrinsic and extrinsic TLS.[26] The extrinsic TLS may be related to extrinsic defects like OH-impurities. Actually, comparing Suprasil I (1250 ppm OH-impurities) with Suprasil W (¡ 5 ppm OH-impurities) the experimentally determined

number of TLS is nearly twice as high. This may be related to the additional contribution of extrinsic TLS.[26] For the intrinsic TLS two different contributions may be of relevance. First, they may be related to TLS where *intrinsic* defects of the silica system are involved. They are characterized by non-tetrahedral local coordination like non-bridging oxygen atoms. Second, intrinsic TLS may also be present in defect-free silica configurations which recently have been analyzed in Ref.[25]. Intuitively, one might expect that defective configurations (intrinsic and extrinsic) are more efficient to locally reorganize and thus to form TLS. Both, the presence of intrinsic and extrinsic defects, will be relevant for a closer rationalization of the low-temperature anomalies in systems like Suprasil.

In previous work on a BMLJ system the properties of extrinsic defects have been analyzed in detail.[27] For this purpose one has included a test Lennard-Jones particle with variable radius and analyzed the DWP, related to this particle. Some dramatic effects have been observed when analyzing a test particle with a radius which is e.g. 25% smaller than the radius of the smaller component of the BMLJ system (data compared with the properties of the majority component): (i) the probability for the formation of a DWP has increased by a factor of approx. 50, (ii) the number of particles, involved in the DWP, has decreased by more than a factor of 2, (iii) the average saddle height of the DWP has increased by a factor of nearly 2, (iv) the deformation potential has decreased by 25%.

In this work we explicitly compare the nature of the TLS of defect-free silica with those of silica containing intrinsic defects and/or extrinsic defects, modelled by a small concentration of Li_2O. It will turn out that all types of TLS have very different properties. On a qualitative level, many features for the extrinsic defects will turns out to be similar to what has been observed for the test particle in the BMLJ system, as sketched above. To underline the interpretation of the results, we compare them with the respective observations for the BMLJ system and with experimental data.

TECHNICAL

The molecular dynamics (MD) simulations have been conducted under NVE-conditions. The velocity Verlet scheme has been chosen to propagate the particles in time. The MD simulations were basically used to generate large numbers of independent structure, which then were analyzed for the occurrence of DWP. Periodic boundary conditions have been

applied.

Binary mixture Lennard-Jones

As a LJ-model glass former we chose a binary mixture system with 80% large A-particles and 20% small B-particles (BMLJ).[28–31] It is supposed to represent NiP (80% ^{62}Ni; 20% ^{31}P) but with a 20% higher particle density.[32] This system was first used by Kob and Anderson. The used potential is of the type

$$V_{\alpha\beta} = 4 \cdot \epsilon_{\alpha\beta}[(\sigma_{\alpha\beta}/r)^{12} - (\sigma_{\alpha\beta}/r)^{6}] + (a + b \cdot r), \tag{1}$$

with $\sigma_{AB} = 0.8\sigma_{AA}$, $\sigma_{BB} = 0.88\sigma_{AA}$, $\epsilon_{AB} = 1.5\epsilon_{AA}$, $\epsilon_{BB} = 0.5\epsilon_{AA}$, $m_B = 0.5m_A$. A linear function $a + b \cdot r$ was added to ensure continuous energies and forces at the cutoff $r_c = 1.8$. The units of length, mass and energy are σ_{AA}, m_A, ϵ_{AA}, the time step within these units was set to 0.01. For the case of NiP the energy unit corresponds to 934 K and σ_{AA} is 2.2 Å. The presented data are taken from our smallest simulated system with 65 particles. The finite size effects have already been analyzed in Ref.[16,17] and are small enough to be neglected.

Silica

The pure silica system has been modeled by the BKS-potential.[33] We have analyzed system sizes of N=150 and N=600 particles. If not mentioned otherwise the data in this work refer to $N = 150$. The system has the standard density of 2.3 g/cm^3 and a short-range cutoff of the BKS-potential of 8.5 Å. The starting configurations for the systematic search correspond to equilibrium configurations at 3000 K, which subsequently were minimized. We have obtained starting structures with and without intrinsic defects, i.e. deviations from a perfect tetrahedral coordination. Due to the fact, that defect related DWP may be relevant, though the number of defects is very small,[34] we do not only analyze the defect free DWP but also the defect related DWP.

To define the coordination of a silicon atom in a classical pair potential it is necessary to introduce maximum bond cutoffs to determine if a bond exists or not. The minimum between the first and the second nn-shell in the radial distribution functions for the minimized structures lies around 2.2Å. This value has thus been used as a cutoff to define bonds, Si–O

distances below this value are considered bonds and larger distances are not. The general results do not critically depend on the used cutoff value as a broad minimum region between the two nearest-neighbor-shells exists.

Lithium silicate

For the alkali silica simulations a 153 particle system with only 2 Li-atoms has been used. The low lithium concentration guarantees, that the Li-atoms behave almost independently and that the network structure is rather similar to that of pure silica. The potential has been taken from Habasaki and Okada.[35] Its alkali-free limit is close to the BKS-potential. The simulations have been conducted under the same conditions as for pure silica.

Search for DWP

The key idea of our search algorithm is to start from one minimized configuration, i.e. a local minimum of the PEL, and then to perform a specified number of MD steps. Afterwards the system is minimized again. When this procedure ends in a configuration which is different from the starting configuration it is checked whether there exists a saddle point between both configurations. If yes, one has identified one DWP. This procedure is repeated many times (typically: 100 times) in order to identify most if not all DWP. A DWP is characterized by three parameters: its asymmetry Δ, its potential height V and its distance between both minima d. More specifically we either use the Euclidean distance d or the mass-weighted distance d_{mwrp} along the reaction path.[16] Since these differences are not relevant in the context of the present work they will be neglected in what follows. For the determination of the saddle a robust saddle search routine has been chosen.[31]

A DWP is kept for the further analysis if $\Delta < \Delta_{max}$ and $d < d_{max}$ where Δ_{max} and d_{max} are specified values. This limitation is essential to enable a systematic search. DWP with, e.g., very large values of the asymmetry are difficult to find such that a systematic search of *all* DWP (starting from a given configuration) is not possible within reasonable computer time. In contrast, if one is only interested in DWP within the range, specified above, one may hope to find (nearly) all DWP. As will be shown below, the TLS are confined to this range, i.e. TLS with $d > d_{max}$ are irrelevant.

A simple way to estimate the degree of completeness of the search procedure is to analyze how often a specific DWP is found during the repeated simulations. It has been shown that for appropriately chosen parameters a systematic search for DWP is indeed possible for the BMLJ system [16] as well as for silica [25] and properties of TLS, i.e. of nearly symmetric DWP, can be extracted. For a successful assessment of TLS properties one first has to deal with the strong positive correlations among all three parameters d, V, and Δ. Guided by the soft-potential model [36,37] we have mapped the distribution $p(d, V, \Delta)$ on a distribution of soft-potential parameters w_2, w_3, w_4 which fortunately to a very approximation turn out to be independent of each other. Based on the independent distribution functions $p_i(w_i)$ it is possible to generate a sufficiently large set of DWP with the same statistical properties as the initial set of DWP. In this way one can cover the full parameter range with high precision and in particular obtain the distribution of TLS as a subset of the whole parameter range. A closer description of this *parametrization method* as well as further technical details can be found in Refs.[16,17].

The parameters, used for our simulations, are given in Tab.1. For the characterization of the DWP we first determine which particle moves most during the transition. This particle is denoted *central* particle. For BMLJ we have therefore distinguished A-type DWP where the central particle is an A-particle and, analogously, B-type DWP. For silica we have defined $\mathrm{DWP^{ND}}$ as the subset of DWP where the initial and the final configuration are defect-free and no bond breaking occurs during the transition. The remaining set is denoted $\mathrm{DWP^{WD}}$. For lithium silicate we define $\mathrm{DWP^{Li}}$ as those DWP for which one of the two lithium atoms is the central particle. The number of DWP, found in our simulations, are also listed in Tab.1.

RESULTS

Properties of DWP parameters

Before analyzing the total number of DWP, found in our simulations with the choice of Δ_{max} and d_{max} as listed in Tab.I, one has to ask whether or not the search for DWP was complete. In Fig.1 we display the results for $\mathrm{DWP^{ND}}$ and $\mathrm{DWP^{WD}}$ when applying the completeness criterion. The curve for $\mathrm{DWP^{ND}}$ behaves similarly to what we have found

	# DWP	d_{max}	Δ_{max}
BMLJ (A-type)	521	0.8	0.5
BMLJ (B-type)	6001	0.8	0.5
DWP^{ND}	250	5 Å	1500 K
DWP^{WD}	1419	”	”
DWP^{Li}	1885	”	”

Table I: The number of DWP analyzed for all different systems (system sizes: N=65 for BMLJ; N=150 for silica; N=153 for lithium silica). They were recorded if their values of d and Δ satisfy $d < d_{max}$ and $\Delta < \Delta_{max}$, respectively.

for the BMLJ system.[16] It displays a maximum for a value much larger than one (here: approx. 30). Qualitatively, this means that whenever a DWP is present it is found quite often during the repeated runs. As a consequence it is statistically very unlikely that a DWP is not found at all. This is exactly the condition for a (nearly) complete search. This result has been already used in our previously published work.[25] In contrast, the probability that a DWP^{WD} is found just once out of the 100 attempts is significantly larger than to be found twice or even more often. Thus, it is likely that several DWP^{WD} are not found at all. A similar observation is made for the DWP^{Li} (data not shown). It is, however, unlikely that the true number of DWP is orders of magnitude larger than the number of DWP already found because otherwise the probability to find a DWP only once or twice would be much larger than 30% for DWP^{WD}. Furthermore for the estimation of the TLS one mainly needs to have reliable information about DWP which are nearly symmetric and have a small value of d (see below for more details). It is likely that this subset of DWP is found with a higher probability because of its proximity on the PEL which further supports that at least the number of TLS, estimated below, is not far away from the true value.

Based on the number of DWP, found in our simulations and listed in Tab.I, and the number of analyzed initial configurations one can estimate the probability that a given configuration contains one DWP within the specified parameter range. For atomic systems like BMLJ it is useful to divide the number of DWP also by the number of particles per configuration to obtain a per-particle DWP probability. Thus, for the A-Type DWP we have defined the probability relative to the number of A-particles. The B-type DWP are treated

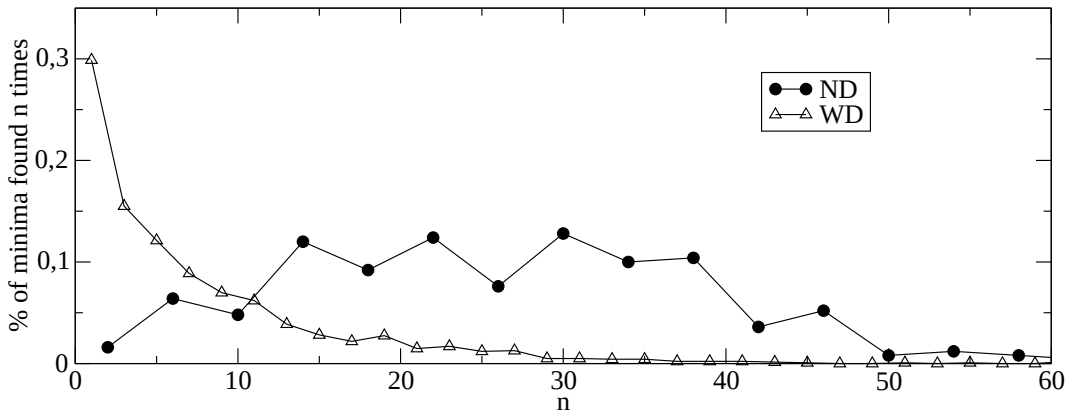

Figure 1: The histogram of how often a nearby minimum was found per starting minimum, using 100 independent runs.

analogously. For the lithium silicate system we consider the occurrence of $\mathrm{DWP}^{\mathrm{Li}}$ relative to the two individual lithium atoms per configuration. For pure silica a SiO_4-tetrahedron serves as an elementary unit because of its rigid character at low temperatures. Thus a silica configuration with $N = 150$ particle contains 50 individual elementary units. Actually, in some models of silica the tetrahedra are directly treated as rigid bodies.[18] We note in passing that the size of the elementary unit can be estimated from analyzing the material constants of silica.[38] Therefore, for a better comparison with other systems the number of $\mathrm{DWP}^{\mathrm{ND}}$ for defect-free configurations is related to the number of tetrahedra. It turns out that for a silica configuration with $N = 150$ atoms the probability to find a DWP is 10 times larger if the configuration contains a defect. Thus the DWP can be to a good approximation exclusively related to the presence of a defect. On average, it turns out that for $N = 150$ a configuration contains approx. 1.2 independent defects. Using all these pieces of information one can express the number of $\mathrm{DWP}^{\mathrm{WD}}$ relative to the number of elementary units, which here are the number of independent defects. For all five different types of DWP the probability of DWP formation per elementary unit (within the specified range of parameters) is given in Tab.II. Note that for $\mathrm{DWP}^{\mathrm{WD}}$ and $\mathrm{DWP}^{\mathrm{Li}}$ we can only determine lower limits.

For understanding the low-temperature anomalies one is interested in the number of TLS (here defined via $\Delta < 2$ K) rather than in the number of DWP. In analogy to the DWP we define the $\mathrm{TLS}^{\mathrm{ND}}$, $\mathrm{TLS}^{\mathrm{WD}}$ and $\mathrm{TLS}^{\mathrm{Li}}$. If the distribution of asymmetries were constant in the interval $[0, \Delta_{max}]$ the number of DWP with an asymmetry smaller 2K could be

	DWP/elem.unit	f_Δ	TLS/elem.unit
BMLJ (A-type)	$1.0 \cdot 10^{-3}$	2.6	$1.1 \cdot 10^{-5}$
BMLJ (B-type)	$4.0 \cdot 10^{-2}$	2.6	$5 \cdot 10^{-4}$
$\mathrm{DWP^{ND}}$	$1.4 \cdot 10^{-3}$	2.0	$3.8 \cdot 10^{-6}$
$\mathrm{DWP^{WD}}$	$\geq 5 \cdot 10^{-1}$	1.1	$\geq 7.3 \cdot 10^{-4}$
$\mathrm{DWP^{Li}}$	$\geq 2.8 \cdot 10^{-1}$	1.25	$\geq 4.7 \cdot 10^{-4}$

Table II: The probability that a specific elementary unit is the central unit for the transition of a DWP with asymmetry less than 2K, i.e. a TLS. f_Δ characterizes the deviations from a constant distribution of asymmetries.

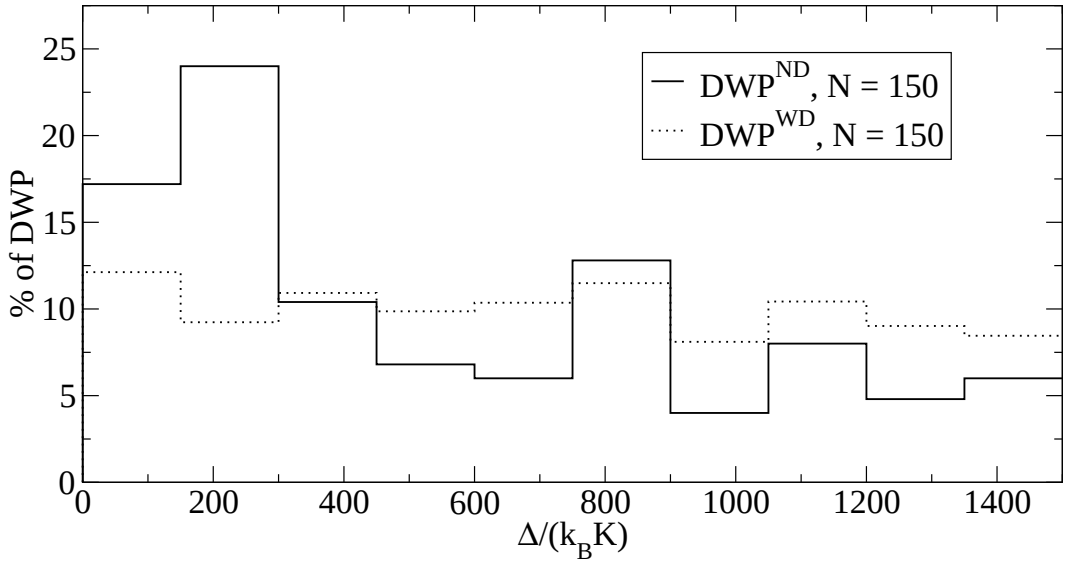

Figure 2: The distribution of asymmetries for the $\mathrm{DWP^{ND}}$ and $\mathrm{DWP^{WD}}$.

directly calculated by multiplying the above values with $2\mathrm{K}/\Delta_{max}$. Closer inspection of the distribution shows, however, that the density is somewhat higher for very small asymmetries; see Fig.2 for $\mathrm{DWP^{ND}}$ and $\mathrm{DWP^{WD}}$. The density for $\Delta < 300$ K is roughly constant within statistical noise. One can define a factor f_Δ which describes the increases of the density in the limit of low asymmetries as compared to the prediction for constant density in the whole interval. An estimation for this value is also shown in Tab.II. As can be judged from Fig.2 there is some statistical uncertainty of approx. 20%. The value of f_Δ is particularly large for $\mathrm{DWP^{ND}}$ and the DWP in the BMLJ system. Qualitatively, it is related to the barrier distribution in Fig.3. Due to the strong correlation of asymmetry and barrier height

DWP very high barrier heights are very unlikely to have a small asymmetry. Thus a broad distribution of barrier heights implies that only a smaller fraction of DWP can be relevant for the low-temperature anomalies. Indeed, it turns out that to a good approximation the value of f_Δ is proportional to the fraction of DWP with $\Delta < 1000$ K in Fig.3. Now the number of TLS per elementary unit can be directly estimated. The results are also given in Tab.II.

As a main conclusion from this analysis it turns out that A-type DWP for the BMLJ system and $\mathrm{DWP^{ND}}$ are very rare. The other extreme are the extrinsic lithium defects $\mathrm{DWP^{Li}}$ as well as the intrinsic defects $\mathrm{DWP^{WD}}$ in silica. Thus the presence of a small particle in a disordered network or the breaking of this network, e.g. via non-bridging oxygens (see below), prompts the formation of bistable modes, i.e. DWP. Hence via local motion of the defect the system can acquire a new metastable position. Also the probability of the formation of B-type DWP for BMLJ is dramatically enhanced. This is consistent with the view that the B-particles can be regarded as defects among the majority of the A-particles. We note in passing that for the lithium silicate system also the number of DWP with silicon or oxygen as central particles is increased by approx. 50% if compared to the number of DWP for an average silica configuration. This may be related to the fact that the presence of lithium automatically implies a breaking of the silicate network and then the additional intrinsic defects may give rise to an increased number of DWP.

A central DWP parameter is the barrier height. In Fig.3 we display the distribution of barriers for the different types of DWP. Interestingly, the absolute values of the barrier heights are very different. For $\mathrm{DWP^{ND}}$ the transition between both minima can be described as a coupled rotation of several SiO_4-tetrahedra.[25] Obviously, this can be achieved by surmounting only a relatively small energy barrier. A rationalization for the higher barriers for $\mathrm{DWP^{WD}}$ and $\mathrm{DWP^{Li}}$ will be presented further below. In Ref.[39] the distribution for $\mathrm{DWP^{ND}}$ has been estimated to be confined to approx. $V < 1000$ K. This is in very good agreement with the data shown in Fig.3.

Furthermore, one may ask whether the properties of the DWP depend on the energy of the starting configuration. Therefore we analyze the average barrier height of the DWP in dependence of this initial energy; see Fig.4. The energies correspond to the relevant energies at low temperatures. Actually, the previous analysis about the relaxation properties of silica has revealed that the PEL of silica has a low-energy cutoff which for the present

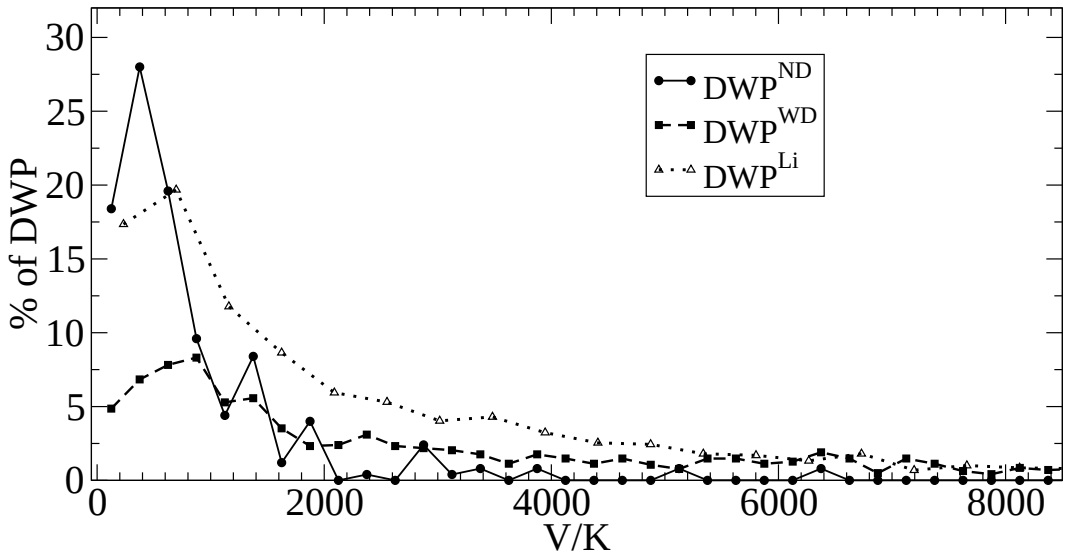

Figure 3: Barrier distribution for the different types of DWP.

system size can be estimated to be around -2895 eV.[40] For all three systems there is no significant dependence of the average potential height on energy relative to the level of statistical uncertainties. Thus, one may conclude in analogy to our previous results for the BMLJ system, that the fast cooling rate in computer simulations is no serious problem for the quantitative analysis of DWP. Also different quantities, analyzed along this line, do not show a significant energy-dependence.

Finally, we have analyzed the distance d between the two minima of the DWP. The results are shown in Fig.5. Nearly all DWP^{ND} display distances between 1.5 Å and 4 Å. This implies that the motional pattern of coupled rotations of tetrahedra requires, on the one hand, some minimum length and, on the other hand, does not extend beyond some upper limit. In contrast, in particular for the defect dynamics, i.e. DWP^{WD} a larger variance of possible distances is observed. This hints towards a larger number of different motional mechanisms in the presence of defects.

Microscopic properties of DWP

A central question deals with the number of atoms involved in the transition. This can be captured by the participation ratio. In literature different definitions can be found. Here we use R^H and R^S as defined in Tab.III. d_{max} is the distance moved by the central particle

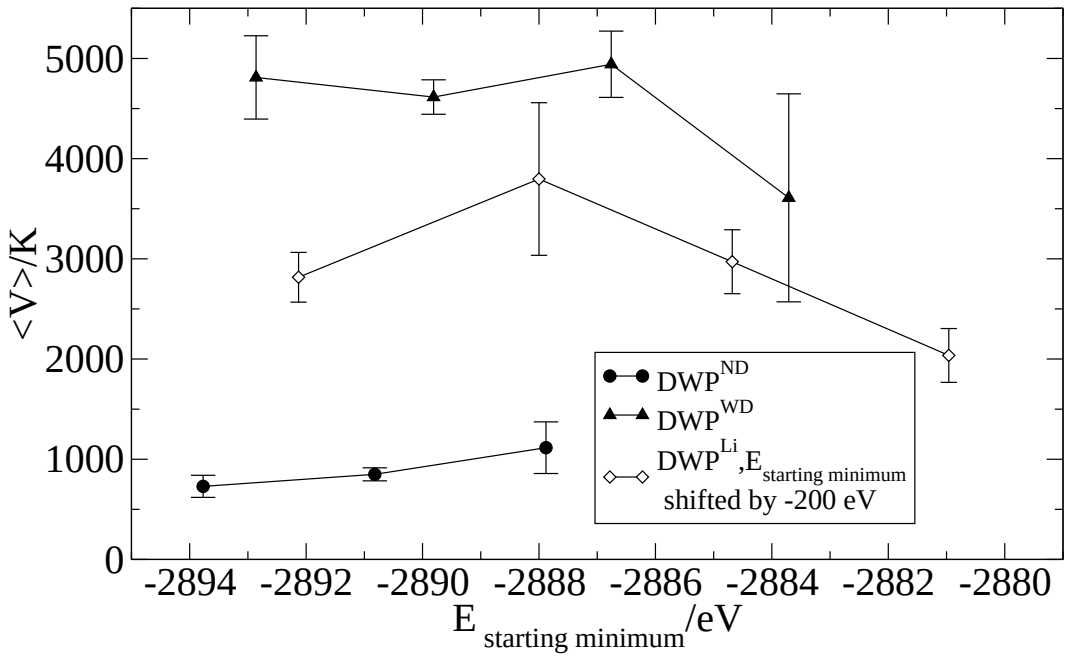

Figure 4: Dependence of the average DWP barrier on the energy of the initial configuration. The $\mathrm{DWP^{Li}}$ data are shifted by -200 eV to handle the different minimum energies.

	R^H $\langle d^2/d^2_{\max}\rangle$	R^S $d^4/\sum_i d_i^4$
BMLJ (A-type)	6.7	16.1
BMLJ (B-type)	3.0	9.0
$\mathrm{DWP^{ND}}$, $N = 150$	9.1	24
$\mathrm{DWP^{ND}}$, $N = 600$	9.0	31
$\mathrm{DWP^{WD}}$, $N = 150$	6.4	19
$\mathrm{DWP^{Li}}$, $N = 153$	1.9	3.6

Table III: Participation ratios for the different systems studied in this work.

and d_i the distance moved by the i-th particle. The results are listed in Tab.III.

As the most prominent feature the transition in $\mathrm{DWP^{Li}}$ is extremely localized. Thus one may speak of a single-particle transition. This agrees with our previous observation for the BMLJ system. There the B-type DWP, corresponding to the dynamics of the small B-particles, are localized, too. In contrast, larger participation ratios can be found for the A-type DWP in the BMLJ system as well as the DWP in the silica system. Similar values

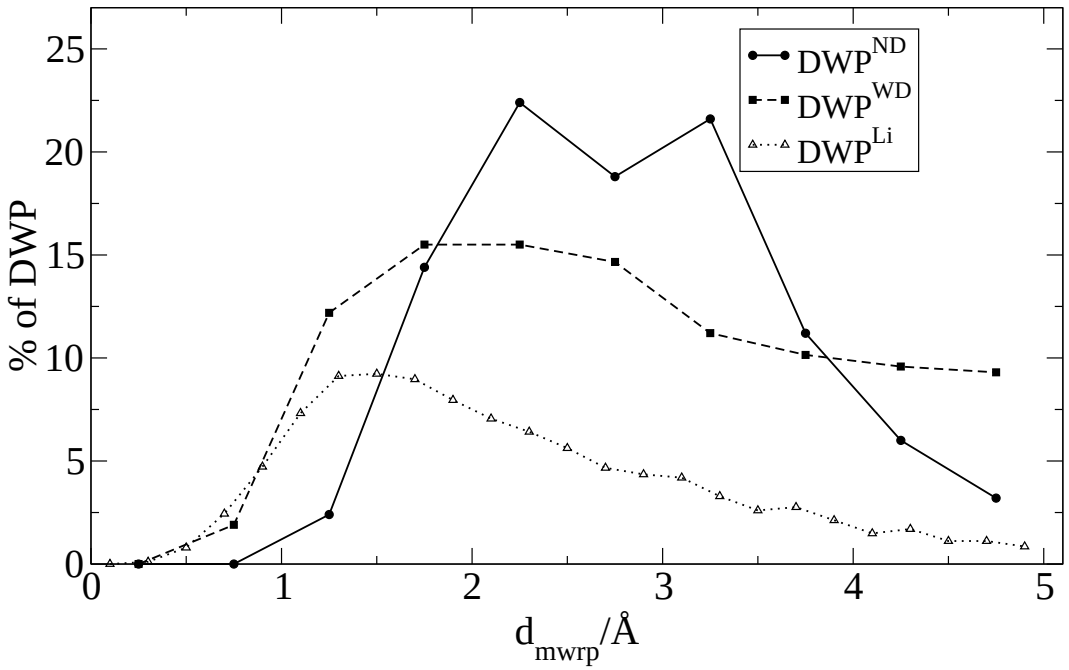

Figure 5: The distribution of distances for different DWP.

have been obtained in Refs.[19,41]. Taking into account that for silica the elementary units are SiO_4 tetrahedra and not individual atoms, these values should be considered as upper limits for the number of independent degrees of freedom, involved in the transitions. For DWP^{ND} we have performed a systematic search for $N = 150$ and $N = 600$ particles. In agreement with other observables finite size effects are only weak. Thus, one may conclude that neither the finite size of our sample nor the fast quenching rate, used in computer simulations, have a relevant effect on the properties of the DWP.

For the case of the BMLJ system the participation ratio is slightly lower for DWP with smaller distances d (unpublished work). Since TLS have smaller distances than the average DWP, the above values for the participation ratio should be regarded as upper limits for TLS. Thus, one may conclude that in all cases one has less than, let‘s say, 10 particles which participate in a tunneling mode.

For a closer analysis of the nature of the transitions we have analyzed whether the transition between both minima for the different particles is basically a straight line in real space or whether it is strongly curved. For this study we compare for all particles the transition vector from the first minimum to the saddle with the corresponding vector from the saddle to the second minimum and determine the angle α between both vectors. In case of

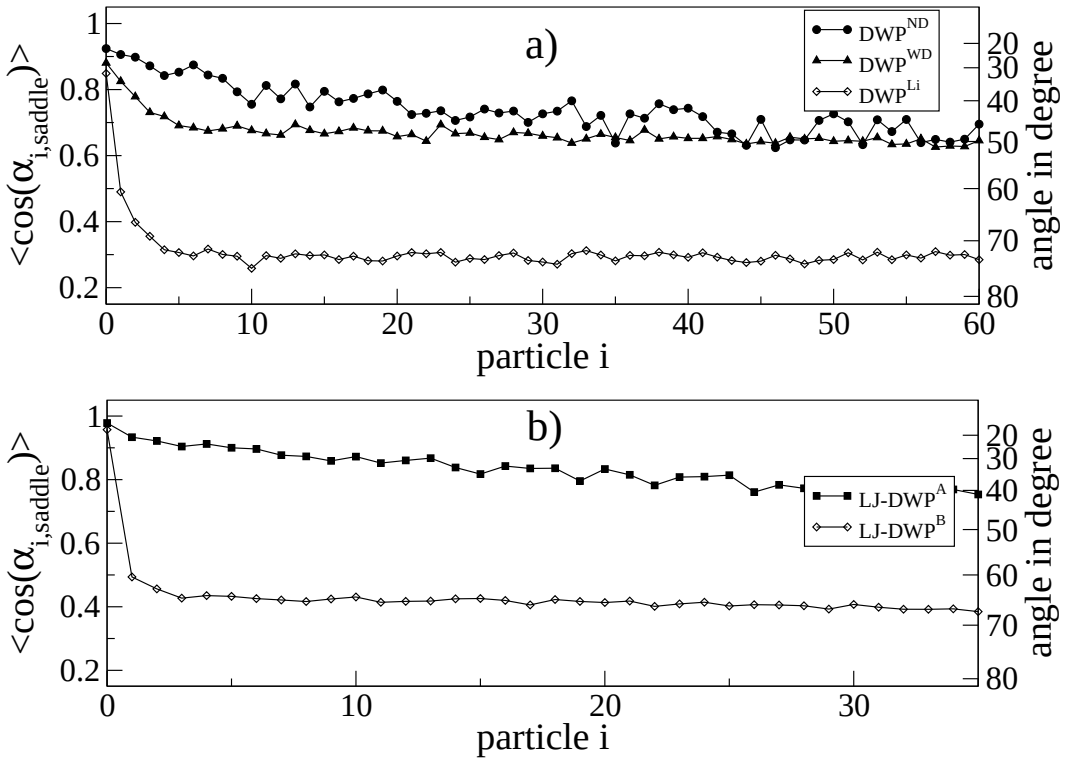

Figure 6: The average cosine of the angle between the transitions from the first minimum to the saddle and the transition from saddle to the second minimum. The particles are sorted according to their absolute value of the Euclidean distance when moving between both minimum configurations.

a straight line both vectors are parallel, i.e. $\alpha = 0$. In the other extreme case a particle performs a forward-backward motion such that both vectors are antiparallel, i.e. $\alpha = \pi$. Furthermore, we sort the particles according to the Euclidean distance between the initial and final position. The particle with index $i = 0$ thus corresponds to the central particle, the particle with index $i = 1$ to the particles moving second most and so on. This allows us to average over all DWP. The results are shown in Fig.6.

Clearly, for all systems the central particle of a DWP moves along a nearly straight line during the transition ($\langle \cos \alpha \rangle \approx 0.9$). However, for the other particles major differences exist. For A-type DWP of the BMLJ system all particles perform a relatively straight transition path. This reflects the cooperative nature of the transition. In contrast, for B-type DWP already the transition path for the particle with $i = 1$ displays a strong curvature. This is compatible with the single-particle nature of the DWP. During the transition of a small B-particle between two local minima of the PEL the surrounding A-particles mainly retreat

during the transition thereby reducing the value of the saddle energy and finally go back to a similar position as before.

Not surprisingly, the same difference is observed when comparing $\mathrm{DWP}^{\mathrm{ND}}$ and $\mathrm{DWP}^{\mathrm{WD}}$ with $\mathrm{DWP}^{\mathrm{Li}}$. The one-particle type transitions for $\mathrm{DWP}^{\mathrm{Li}}$ are, in analogy to the B-type DWP, connected with a strong curvature for the transition of the remaining particles. There are, however, additional differences between $\mathrm{DWP}^{\mathrm{ND}}$ and $\mathrm{DWP}^{\mathrm{WD}}$ for small particle index i. The coupled tetrahedra-rotation for $\mathrm{DWP}^{\mathrm{ND}}$ implies a similar behavior of the most mobile particles. In contrast, for the transitions involving defects the degree of cooperativity is somewhat smaller.

Comparing $\mathrm{DWP}^{\mathrm{ND}}$ with the A-type DWP from the BMLJ system it turns out that that the angles are generally larger in the silica system. The motion is thus more curved, which seems reasonable due to the network structure and fits to displacements due to rotating tetrahedra.

Microscopic mechanism of the DWP transition

In Ref.[25] it has been shown that for $\mathrm{DWP}^{\mathrm{ND}}$ the crucial step during the transition is a Si-O-Si bond flip. Correspondingly, in more than 99% of all cases the central particle is an oxygen and only starting from particle index $i = 10$ (see above for its definition) the probability to find a silicon atom is close to the statistical value of 1/3. Qualitatively, the dominance of oxygen atoms as the most displaced particle is compatible with the picture of cooperative tetrahedra rotations which mainly involve the dynamics of oxygen atoms. Interestingly, it turns out that oxygen atoms, acting as central atoms, possess a significantly shorter Si-O bond length. This structural motif seems to enhance the probability for the formation of a DWP.[25]

No simple picture for $\mathrm{DWP}^{\mathrm{WD}}$ can be formulated. Rather we have observed a variety of different mechanisms from a close inspection of 30 DWP. Most of the times the transition could be described by one of the following three mechanisms: (1) A bond between a silicon and a threefold coordinated oxygen breaks, the silicon forms a new bond with another oxygen. This oxygen is now threefold coordinated. (2) A bond with a threefold coordinated oxygen breaks and a silicon center changes its coordination from four to three or from five to four. (3) A dangling oxygen (coordinated to only one silicon) forms a bond to a three- or

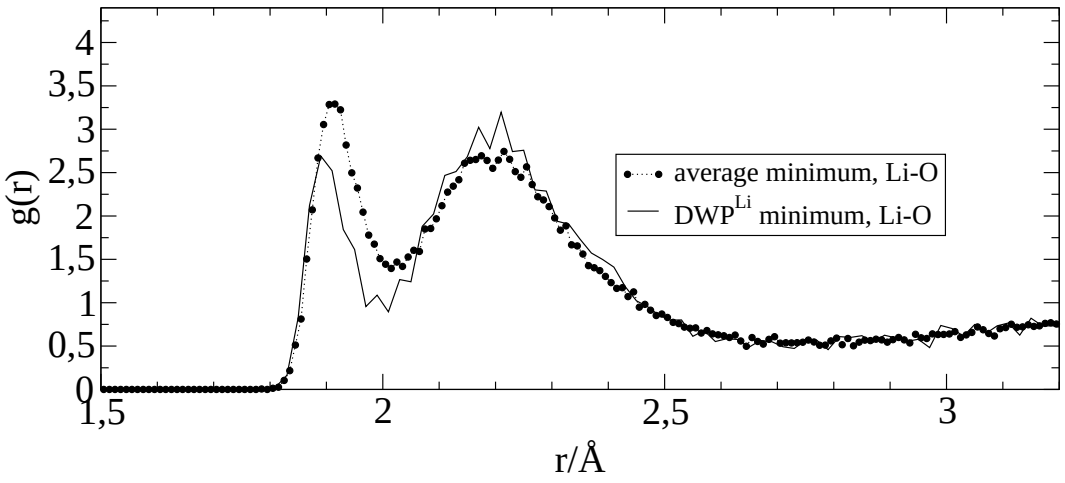

Figure 7: Partial pair correlation function $g_{Li-O}(r)$ for the central lithium of the DWP^{Li} in comparison with the average radial distribution function. Only the first peak is shown as no differences exist in other sections.

fourfold coordinated silicon resulting in a four- or fivefold coordinated silicon and sometimes another oxygen from that silicon becomes either a dangling oxygen itself or coordinates to another silicon. The variety of these scenarios in part also reflects the different types of DWP. Not surprisingly, in this case the probability that the central particle is an oxygen atom is only slightly enhanced as compared to the statistical value (75%).

To study the case of DWP^{Li} we have analyzed the partial Li-O pair correlation function for the minimum configuration. The results for the nearest-neighbor shell are shown in Fig.7. The first peak of this double-peak structure is mainly related to non-bridging oxygen the second peak to bridging oxygen. The density of oxygen atoms, related to the first peak (and thus being mainly non-bridging oxygen), is decreased by approx. 25% when a DWP is present. The integration of both peaks shows that density is transferred from the first to the second peak, but no density is lost from the first two peaks. Thus a reduction of the density of non-bridging oxygen and a corresponding increase of the number of bridging oxygen is a prerequisite for the formation of a DWP. Interestingly, the average number of oxygen atoms in the nearest-neighbor shell decreases from 3.9 to 3.4 when comparing the minimum with the saddle. Thus, during the transition the lithium ion changes part of its oxygen neighborhood.

Dipole Moment

Of major experimental interest is the coupling of the TLS to electric fields via their dipole moment. It can be easily determined via

$$\vec{M} = \sum_i q_i \vec{d}_i \tag{2}$$

where q_i denotes the partial charge and $\vec{d}_i$ the translational vector of particle i during the transition. Of interest is the absolute value of the dipole moment $M = \sqrt{|\vec{M}|^2}$ which can be calculated in a straightforward manner from Eq.2. More precisely, we have averaged M^2 and finally calculated the square root. The partial charges in our potentials are 0.87e for lithium, 2.4e for silicon and -1.2e for oxygen. Note that a single-particle transition with $d = 1$Å and unit charge would correspond to 4.8 Debye. The results are shown in Fig.8 for the different types of DWP. We have averaged DWP with similar distances d, in order to keep track of a possible dependence on d. To a good approximation the data can be described by a linear relation, i.e.

$$M = \zeta q d \tag{3}$$

where q is the average partial charge and ζ a dimensionless proportionality constant. In order to convey a feeling for the absolute value of M it may be instructive to estimate M for the simple scenario for which all particles move independently, i.e. the $\vec{d}_i$ are uncorrelated. In this limit one obtains the same expression as Eq.3 with $\zeta = 1$. Thus the proportionality to d is a generic property which results from the definition of the dipole moment whereas the value of ζ contains information about the motional mechanism.

For $\mathrm{DWP^{Li}}$ one would expect $M(2\text{Å}) \approx 8$D (using the partial charge of lithium) which is close to the numerically found value. Thus we find $\zeta \approx 1$. In any event, for a localized transition any correlation effects between adjacent particles cannot be relevant for the dipole moment. The other extreme case is $\mathrm{DWP^{ND}}$ for which the dipole moment is approx. 10 times smaller than expected for the uncorrelated case. This clearly shows that the dynamics is highly cooperative. In general, two effects may give rise to the reduction. First, particles of opposite charge move in the same direction; second, identical particles move in opposite directions. The latter case is relevant for $\mathrm{DWP^{ND}}$ because of the dominance of tetrahedra rotations, involving significant oxygen motion. In case of ideal rotations around a threefold

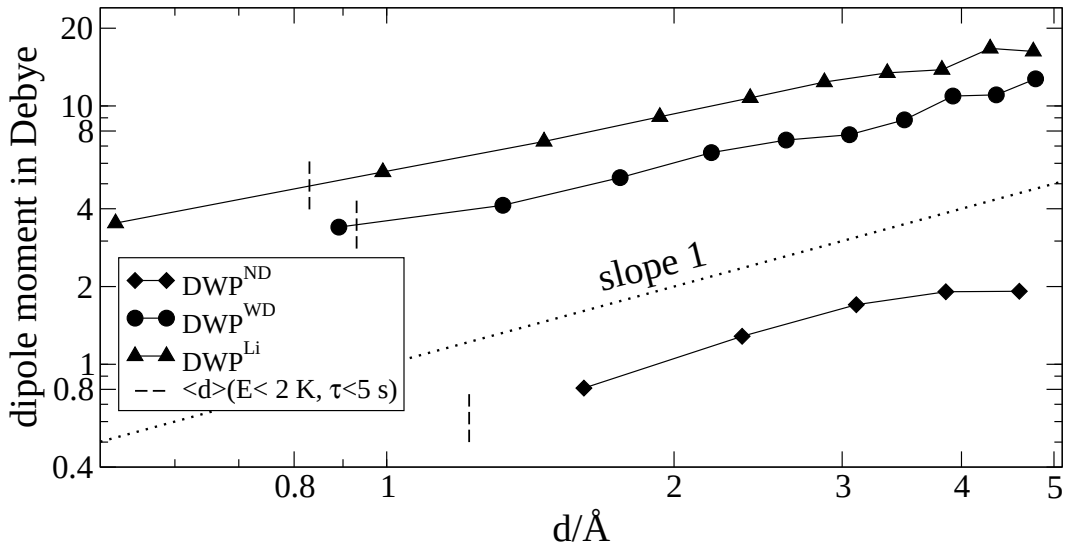

Figure 8: The dipole moment for DWP^{ND} DWP^{WD} and DWP^{Li} in dependence of the distance between both minima. Included is a line of slope 1 and the average distances, estimated for the TLS.

axis the resulting dipole moment would be zero. Due to the non-symmetric nature of the actual rotational axis some residual dipole moment remains.[25]

For DWP^{WD} the reduction as compared to the statistical value is only a factor of approx. 3 (taking into account the somewhat higher effective charge because also silicon atoms can move significantly). Despite the similarity in the participation ratios of DWP^{ND} and DWP^{WD} this shows that the nature of the cooperativity is significantly different. Beyond the rotation of tetrahedra it is the transfer of the defect structure which plays an essential role and which does not possess the cancelation effect of pure tetrahedral rotations.

For comparison with experimentally determined dipole moments one has to take into account the dependence on the distance between both minima of the DWP. As already discussed above the distance for TLS is much smaller than that for the average DWP found in our simulations. This is a direct consequence of the generic correlations between asymmetry and distance. Using the parametrization method, sketched above, it is possible to calculate the distribution of TLS from the distribution of DWP. For the present analysis we are more specific with the definition of TLS. Beyond a near-degeneracy of the lowest two eigenstates (energy difference < 2 K) of the TLS we also require that the relaxation time τ is smaller than 5s.[17] This means that the TLS is active on the time scale of typical experiments.

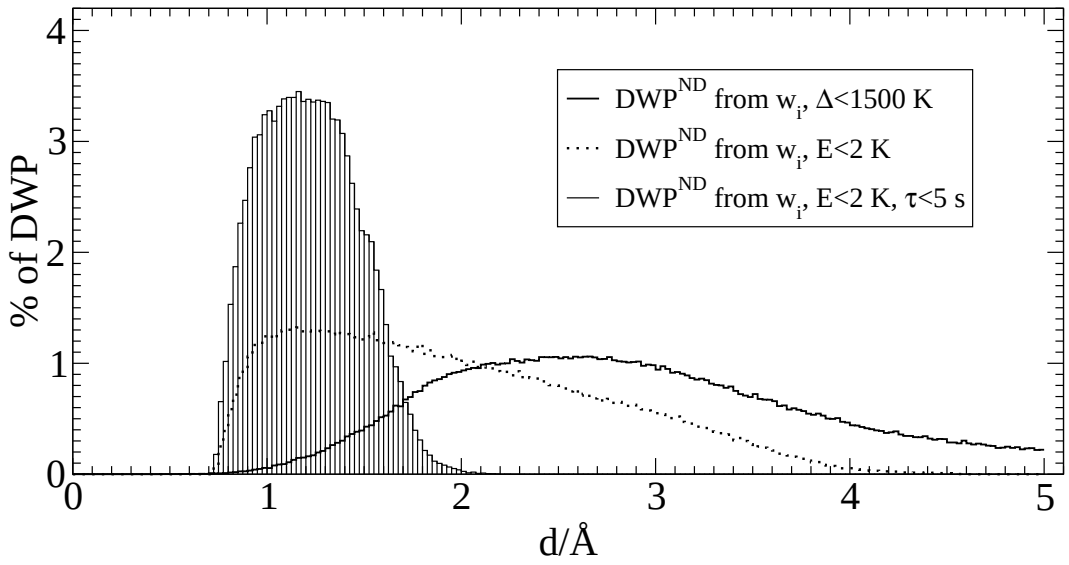

Figure 9: The distance distribution for a subset of $\mathrm{DWP}^{\mathrm{ND}}$ fulfilling different criteria as mentioned in the inset.

	d_{TLS}	ζ	M
$\mathrm{TLS}^{\mathrm{ND}}$	1.20 Å	0.1	0.65 D
$\mathrm{TLS}^{\mathrm{WD}}$	0.93 Å	0.3	3.5 D
$\mathrm{TLS}^{\mathrm{Li}}$	0.83 Å	1.0	5.0 D

Table IV: The dipole moments for the different types of TLS. Included are the reduction factors ζ due to correlated motion of the participating atoms.

This additional criterion in particular excludes DWP with very high barriers and/or large distances. This reduces the values of d for the relevant TLS even further. The results for $\mathrm{DWP}^{\mathrm{ND}}$ are shown in Fig.9.

Using the parametrization method we first have recalculated the distribution of DWP, compatible with our limiting values d_{max}, Δ_{max}. This is the right curve in Fig.9. It is, of course, very similar to the original density distribution in Fig.5. Using the additional restriction $E < 2$ K one obtains a set of DWP which is shifted towards smaller values of d. The final set of DWP with the additional restriction $\tau < 5$s basically excludes DWP with $d > 2$Å. The average distance of these TLS is $d_{TLS} = 1.2$Å. Thus together with Fig.8 one may estimate a dipole moment of 0.65 D (see Tab.IV) for TLS in the non-defect case which is close to the value of 0.6 D, reported in Ref.[26].

We have performed the same analysis for the other two cases. The results for the values of d_{TLS} and the dipole moment are given in Tab.IV. Interestingly, the experimental value for OH-defects is approx. 4 D which is close to the value for TLS^{Li} as well as TLS^{WD}. Thus, it appears that OH-defects and Li-defects have a similar transition mechanism during their tunneling motion.

In recent work Eq.3 has been derived, using a somewhat different notation.[42] The derivation was based on the ideas of the random first order transition theory. The parameter ζ was empirically introduced as a phenomenological constant ($\zeta \approx 0.1$) which is needed to recover the experimentally determined dipole moment of TLS^{ND}. It has been postulated that ζq is the effective partial charge, stemming from a Coulomb charge on a bead, which is much smaller than the electron charge e.[42] In contrast, in the present work we can show that the smallness of ζ can be fully explained by the complex motional mechanism of the TLS transitions in silica.

DISCUSSION AND SUMMARY

Via extended computer simulations we have analyzed the properties of the DWP in silica and lithium silicate. Most importantly, the typical limitations of computer simulations, i.e. finite-time (resulting in fast quenching rates) and finite-size effects, do not hamper the characterization of the DWP within statistical uncertainties. The latter point can be concluded from the fact that the DWP properties do not depend on the energy of the initial glassy configuration and, in general, for small systems the energy is most relevant for predicting the dynamic properties.[31] This is analogous to the case of BMLJ. We should note in passing that for the BMLJ system properties like the vibrational density depend on the energy of the configuration and thus on the cooling rate.[43] In contrast, for silica even the vibrational properties are to a large extent independent of energy.[44] A quantitative estimation of the number of DWP was possible for the BMLJ system and the DWP^{ND}. In contrast, for DWP^{WD} and DWP^{Li} a complete search for DWP was not possible within accessible computer times. However, one could obtain reasonable lower bounds for the number of DWP.

The lithium ions in lithium silicate may be regarded as a prototype system for extrinsic defects, immersed in a pure glass former. The DWP with lithium as central particle, i.e. the

TLS^{Li} mainly correspond to single lithium transitions. On a qualitative level the situation is similar to the case of the small B-particles in the BMLJ system which may be regarded as defects being added to the larger A-particles. Also in this case the average DWP resembles a single-particle transition (this holds even more for a small test particle in the BMLJ system). Furthermore, in both cases the probability to form DWP is significantly higher than in the remaining glass (A-particles in BMLJ and silica in lithium silicate). Thus extrinsic defects are very efficient in prompting the formation of DWP.

The transitions in DWP^{ND} and DWP^{WD} as well as the A-type DWP in the BMLJ system involve the displacement of a somewhat larger number of particles as reflected by larger values of the participation ratio. This spatial extension, however, is still relatively small as compared to some general predictions about the nature of TLS.[5]

A closer analysis shows that DWP^{ND} and DWP^{WD}, i.e. DWP in a configuration without defects and with defects, respectively, behave very differently. The transition dynamics for DWP^{ND} can be characterized as coupled rotations of SiO_4-tetrahedra. In particular this gives rise to a very small value of the dipole moment of this transition, i.e. a very small effective charge transport. In contrast, for DWP^{WD} the dynamics is largely determined by defect-specific modes which effectively give rise to a much larger dipole moment. One may speculate that this is the reason why on average the potential barrier for DWP^{WD} is much larger than that of DWP^{ND}. A significant charge transport involves a major reorganization of the whole system which typically will be connected with a significant activation energy due to the dominant character of the Coulomb energy.

To which degree do our simulations explain the results of low-temperature experiments for vitreous silica?

Defect-free TLS: As already mentioned above we find approx. $4 \cdot 10^{-6}$ TLS/tetrahedron without defects. As discussed in Ref.[25] this translates into an effective density of TLS $\bar{P}$, accessible from acoustic experiments, which within a factor of 3 agrees with the experimentally observed value for Suprasil W.[26]

Dipole moments: The dipole moment for TLS^{ND} is close to the experimental value, obtained for Suprasil W.[26] Increasing the concentration of OH, i.e. using Suprasil I, one obtains a second contribution with a dipole moment which is larger by nearly one order of magnitude.[26] Naturally, it has been related to the tunneling of the OH-impurities. Interestingly, similar dipole moments are observed for TLS^{Li} and TLS^{WD}. Since TLS with such

large dipole moments are absent in Suprasil W one may conclude that TLS^{WD} do not play a major role.

Relevance of intrinsic defects: The previous conclusion can be directly checked by analyzing the estimated number of TLS^{WD}. It would be of the same size as the TLS^{ND} from the undistorted silica network if there exists at least one intrinsic defect per 200 SiO_4-tetrahedra (please have in mind the uncertainty in the determination of the number of DWP^{WD} and DWP^{Li}as discussed above). Analysis of molecular dynamics simulations of silica, using the metabasin approach, suggests that around T_g there is roughly 1 silicon defect per 300 tetrahedra (data not shown). A different way of extrapolation for BKS-data yields a significantly smaller fraction of defects.[34] Furthermore, density functional calculations in general lead to a smaller number of defects than using the BKS-potential.[45] To the best of our knowledge no definite experimental information is available for the number of defects in pure silica. Thus, combining our results for the probability of generating TLS^{WD} with the (somewhat uncertain) absolute number of intrinsic defects, the numerical results are at least consistent with the experimentally observed absence of TLS^{WD} (using the conclusion from above).

Relevance of extrinsic defects: The number of TLS^{Li} would be close to that of TLS^{ND} if there is one lithium ion per 125 tetrahedra. For Suprasil I (1200 ppm OH-defects by weight) one thus has one OH-molecule per 240 SiO_4-tetrahedra. Experimentally it has been found via dielectric echo experiments[26] as well as specific heat experiments[46] that the number of extrinsic TLS is half the number of intrinsic TLS. Thus an equal contribution of extrinsic and intrinsic TLS would require one OH-molecule per 240/2=120 tetrahedra which is close to the value we obtained for an equal contribution of TLS^{Li} to TLS^{ND}. Of course, this perfect agreement is to some extent accidental, given the different nature of lithium and OH-defects and the non-completeness of the search. In any event, the order of magnitude seems to be fully compatible.

Coupling to acoustic modes: It is estimated from experiments that the deformation potential is approx. 40% smaller for extrinsic TLS than for intrinsic TLS (more specifically, TLS^{ND}, according to the discussion above). This result is obtained, first, from the relaxation of electric echoes[26] and, second, from the comparison of the specific heat and the thermal conductivity for Suprasil I and Suprasil W. The difference between both probes is much smaller for the thermal conductivity.[47] It is known from theoretical considerations that the deformation potential scales with the average distance d.[9] The different values of d in Tab.IV

for TLS^{Li} as compared to TLS^{ND} suggest that indeed the deformation potential for extrinsic TLS may be significantly smaller than for intrinsic TLS.

In summary, present-day computer simulations are able to reveal many microscopic properties of two-level systems in glasses in the Kelvin regime and enable a quantitative comparison with experimental data. Via the complementary information from theory and experiments a detailed knowledge about the underlying nature of tunneling systems becomes accessible. In particular the magnetic field dependence of polarization echo experiments may be promising to yield further insight about the microscopic nature of TLS from the experimental side .[48,49] In any case, based on the additional information from this type of simulations the tunneling systems need no longer be considered as phenomenological entities.

We like to thank H. Lammert, A. Saksaengwijit and K. Trachenko for fruitful discussions and the International Graduate School of Chemistry for funding. Furthermore we would like to thank R.J. Silbey for the initial ideas of this project.

[1] Zeller, R. C.; Pohl, R. O. *Phys. Rev. B* **1971**, *4*, 2029.

[2] Phillips, W. A. *J. Low Temp. Phys.* **1972**, *7*, 351.

[3] Anderson, P. W.; Halperin, B. I.; Varma, C. M. *Phil. Mag.* **1972**, *25*, 1.

[4] Kühn, R. *Europhys. Lett.* **2003**, *62*, 313–319.

[5] Lubchenko, V.; Wolynes, P. G. *Phys. Rev. Lett.* **2001**, *87*, 195901.

[6] Guttmann, L.; Rahman, S. M. *Rep. Prog. Phys.* **1987**, *50*, 1657–1708.

[7] Dyadyna, G. A.; Karpov, V. G.; Solovev, V. G.; Khrisanov, V. A. *Sov. phys. Solid State* **1989**, *31*, 629.

[8] Heuer, A.; Silbey, R. J. *Phys. Rev. Lett.* **1993**, *70*, 3911.

[9] Heuer, A.; Silbey, R. J. *Phys. Rev. B* **1993**, *48*, 9411.

[10] Heuer, A.; Silbey, R. J. *Phys. Rev. B* **1997**, *56*, 161.

[11] Heuer, A.; Silbey, R. J. *Phys. Rev. B* **1994**, *49*, 1441.

[12] Heuer, A.; Silbey, R. J. *Phys. Rev. B* **1996**, *55*, 609.

[13] Oligschleger, C.; Schober, H. R. *Solid State Comm.* **1995**, *93*, 1031–1035.

[14] Daldoss, G.; Pilla, O.; Viliani, G.; Brangian, C. *Phys. Rev. B* **1999**, *60*, 3200–3205.

[15] Schober, H. R. *J. of Non-Cryst. Solids* **2002**, *307-310*, 40–49.

[16] Reinisch, J.; Heuer, A. *Phys. Rev. B* **2004**, *70*, 064201.

[17] Reinisch, J.; Heuer, A. *J. Low. Temp. Phys.* **2004**, *137*, 267–287.

[18] Trachenko, K.; Dove, M. T.; Hammonds, K. D.; Harris, M. J.; Heine, V. *Phys. Rev. Lett.* **1998**, *81*, 3431–3434.

[19] Trachenko, K.; Dove, M. T.; Harris, M. J.; Heine, V. *J. Phys.: Condens. Matter* **1998**, *12*, 8041–8064.

[20] Trachenko, K.; Dove, M. T.; Heine, V. *Phys. Rev. B* **2002**, *65*, 092201.

[21] Trachenko, K.; Turlakov, M. *Phys. Rev. B* **2006**, *73*, 012203.

[22] Buchenau, U.; Nücker, N.; Dianoux, A. J. *Phys. Rev. Lett.* **1984**, *53*, 2316–2319.

[23] Taraskin, S.; Elliott, S. *Phys. Rev. B* **1999**, *59*, 8572.

[24] Mousseau, N.; Bakema, G. T.; de Leeuw, S. W. *J. of Chem. Phys.* **2000**, *112*, 960–964.

[25] Reinisch, J.; Heuer, A. *Phys. Rev. Lett.* **2005**, *95*, 155502.

[26] Golding, B.; v. Schickfus, M.; Hunklinger, S.; Dransfeld, K. *Phys. Rev. Lett.* **1979**, *43*, 1817.

[27] Heuer, A.; Neu, P. *J. Chem. Phys.* **1997**, *107*, 8686.

[28] Kob, W.; Andersen, H. C. *Phys. Rev. E.* **1995**, *51*, 4626.

[29] Kob, W. *J. Phys. Condensed Matter* **1999**, *11*, R85.

[30] Broderix, K.; Bhattacharya, K. K.; Cavagna, A.; Zippelius, A.; Giardina, I. *Phys. Rev. Lett.* **2000**, *85*, 5360.

[31] Doliwa, B.; Heuer, A. *Phys. Rev. E* **2003**, *67*, 031506.

[32] Weber, T. A.; Stillinger, F. H. *Phys. Rev. B* **1985**, *31*, 1954–1963.

[33] van Beest, B. W.; Kramer, G. J.; van Santen, R. A. *Phys. Rev. Lett.* **1990**, *64*, 1955–1958.

[34] Horbach, J.; Kob, W. *Phys. Rev. B* **1999**, *60*, 3169.

[35] Habasaki, J.; Okada, I. *Molec. Simul.* **1992**, *9*, 319–326.

[36] Karpov, V. G.; Klinger, M. I.; Ignatiev, F. N. *Sov. Phys. JETP* **1983**, *57*, 439.

[37] Buchenau, U.; Galperin, Y. M.; Gurevich, V. L.; Schober, H. R. *Phys. Rev. B* **1991**, *43*, 5039.

[38] Heuer, A.; Spiess, H. W. *J. Non-Cryst. Solids* **1994**, *176*, 294.

[39] Keil, R.; Kasper, G.; Hunklinger, S. *J. Non-Cryst. Solids* **1993**, *166*, 1183.

[40] Saksaengwijit, A.; Reinisch, J.; Heuer, A. *Phys. Rev. Lett.* **2004**, *93*, 235701.

[41] Ekunwe, N.; Lacks, D. J. *Phys. Rev. B* **2002**, *66*, 212101.

[42] Lubchenko, V.; Silbey, R. J.; Wolynes, P. G. *arXiv: cond-mat/0506735* **2005**.

[43] Büchner, S.; Heuer, A. *Phys. Rev. E* **1999**, *60*, 6507.

[44] Saika-Voivod, I.; Sciortino, F.; Poole, P. H. *Phys. Rev. E.* **2004**, *69*, 041503.

[45] Trachenko, A.; Tangney, P.; Scandolo, S.; Pasquarello, A.; Carr, R. *Phys. Rev. Lett.* **2002**, *89*, 245504.

[46] Liu, X.; Löhneysen, H.; Weiss, G.; Arndt, J. *Z. Phys. B* **1995**, *99*, 49–55.

[47] Hunklinger, S.; Piche, L.; Lasjaunias, J. C.; Dransfeld, K. *J. Phys. C: Solid State Phys.* **1975**, *8*, L423.

[48] Würger, A.; Fleischmann, A.; Enss, C. *Phys. Rev. Lett.* **2002**, *89*, 237601.

[49] Nagel, P.; Fleischmann, A.; Hunklinger, S.; Enss, C. *Phys. Rev. Lett.* **2004**, *92*, 245511.